RSC Advances

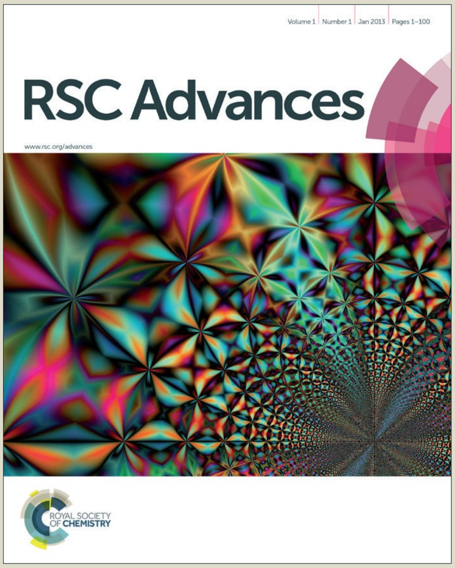

ROYAL SOCIETY
OF CHEMISTRY

www.rsc.org/advances

RSC Advances RSCPublishing

ARTICLE

Cite this: DOI: 10.1039/x0xx00000x

Received 00th January 2012,
Accepted 00th January 2012

DOI: 10.1039/x0xx00000x

www.rsc.org/

Nickel Schiff-base complexes immobilized on boehmite nanoparticles and their application in the oxidation of sulfides and oxidative coupling of thiols as novel and reusable nano organometal catalysts

Arash Ghorbani-Choghamarani,* Bahman Tahmasbi, Fatemeh Arghand and Sara Faryadi

Boehmite nanoparticles were prepared by very simple and inexpensive procedure in water at room temperature using commercially available materials. Two Schiff-base complexes of nickel have been immobilized on the boehmite nanoparticles. These catalysts were characterized by FT-IR spectroscopy, TGA, XRD, BET, UV-DRS, TEM, SEM, EDS and ICP-OES techniques. These compounds were applied as catalyst for the oxidation of sulfides to sulfoxides and oxidative coupling of thiols to disulfides under mild reaction conditions at room temperature. These catalysts were recovered by simple filtration and reused for several times without significant loss of their catalytic efficiency.

---

* Address correspondence to A. Ghorbani-Choghamarani, Department of Chemistry, Ilam University, P.O. Box 69315516, Ilam, Iran; Tel/Fax: +98 841 2227022; E-mail address: arashghch58@yahoo.com or a.ghorbani@mail.ilam.ac.ir

RSC Advances RSCPublishing

ARTICLE

1 Introduction

Solid catalysts have been widely employed as useful, recoverable and recyclable catalysts in organic synthesis [1, 2]. One way to reach this goal is immobilization of homogeneous catalysts on insoluble supports. The catalytic activity of these solid materials could also efficiently increases using nanomaterial support [3]. Because, when the size of the support is decreased to the nanometre scales, the surface area is substantially increased and the support can be evenly dispersed in solution, to form a homogenous emulsion [4]. Therefore, nanocatalysts can be used as bridge to improve the gap between homogeneous and heterogeneous catalysis, preserving the desirable attributes of both systems [5]. One of the novel nanomaterial supports is boehmite (γ-AlOOH) with orthorhombic unit cells, which it is rarely employed as heterogeneous support for the immobilization of homogeneous catalysts [6]. Nanoboehmite have several attractive features, such as stable orthorhombic structure, high specific surface area, non-toxicity, easily and readily available material, thermal and mechanical stability, ease of surface modification, easy and inexpensive procedure of preparation and favourable biocompatibility [7, 8]. Additionally, the surface of nanoboehmite is covered with hydroxyl groups. These surface hydroxyl groups provide valuable sites that can be grafted with various functional groups in order to produce expensive supported-catalysts such as metal complexes [8, 9]. Boehmite has been used as an absorbent, optical material, composite reinforcement material in ceramics, cosmetic products, vaccine adjuvants, starting material in the synthesis of alumina pillared clays and sweep-flocculation for fresh water treatment [5, 10]. Recently, metal complexes of Schiff-bases have been emerged for the development of a variety of catalysts [11] however, for effective and easier recovered, Schiff base compounds have been grafted on heterogeneous supports [12]. Schiff base transition metal complexes are considered as promising candidates because of their excellent catalytic performances in a wide range of organic transformations [13]. Herein, we report new Schiff-base complexes of nickel grafted on boehmite nanoparticles for the oxidation of sulfides to sulfoxides and also oxidative coupling of thiols into corresponding disulfides under mild reaction conditions. Sulfoxides and disulfides are useful in the synthesis of new products and play an important role in various medical and biological applications [14, 15]. For example, omeprazole and the pesticide fipronil are two typical examples of the sulfoxide derivatives in pharmaceutical and fine chemical industries [16]. Likewise, disulfide bond formation is important in peptides, bioactive molecules as well as oil sweetening processes [17, 18]. Disulfides are used in sulfonylation of enolates and other anions and also useful as vulcanizing agents [17-19]. For this reason, many methods including various catalysts and different oxidants have been developed over the years to perform these transformations [14-19]. Concerning the green oxidant, hydrogen peroxide (with only H_2O as a by-product) as an inexpensive and environmentally benign oxidant has been applied for these oxidations [20].

2 Results and discussion

2.1 Catalyst preparation

The catalysts were prepared by the concise route outlined in Scheme 1. Initially, boehmite nanoparticles have been prepared *via* addition of NaOH to the solution of $Al(NO_3)_3.9H_2O$ as source of aluminium at room temperature. Ultimately, boehmite nanoparticles coated with silica using tetraethylorthosilicate (TEOS). Subsequently, the facial silanol groups were functionalized with APTES, and Schiff-base ligands were formed using condensation of 5-bromosalicylaldehyde or salicylaldehyde with terminal amine groups, which grafted on boehmite nanoparticles. Finally, the Ni-Schiff base complexes supported on boehmite nanoparticles (Ni-complex-boehmite) were prepared *via* complexation of BS-Schiff base with $Ni(NO_3)_2.6H_2O$. These nanomaterials have been characterized by transmission electron microscopy (TEM), scanning electron microscopy (SEM), energy-dispersive X-ray spectroscopy (EDS), inductively coupled plasma atomic emission spectroscopy (ICP-OES), Brunauer–Emmett–Teller (BET), UV–vis diffuse reflectance spectra (UV–vis DRS), X-ray diffraction (XRD) thermogravimetric analysis (TGA) and Fourier transform infrared spectroscopy (FT-IR) techniques.

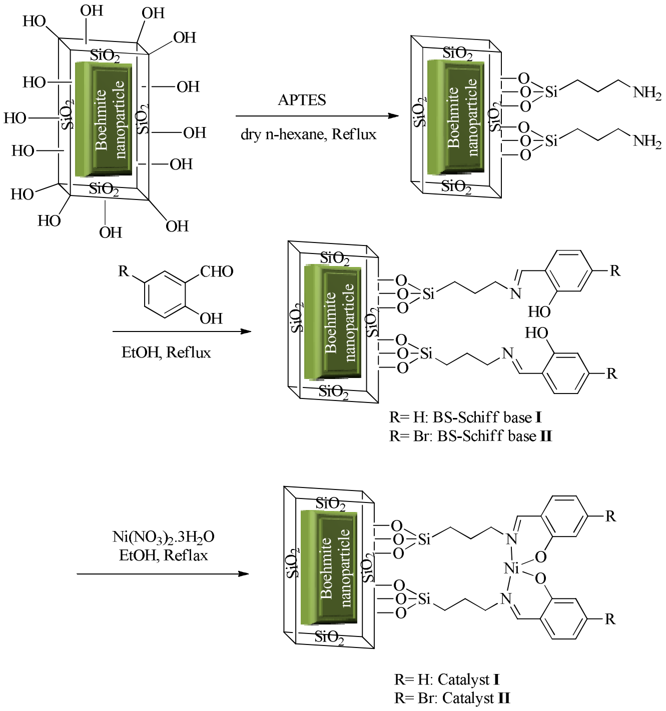

Scheme 1. Synthesis of Ni-complex-boehmite.

2.2 Catalyst characterizations

The size and morphology of boehmite nanoparticles was considered by SEM analysis. The SEM image of boehmite was shown that these nanoparticles were formed of nanometre-sized in quite homogeneous cubic orthorhombic structures (Figure 1a). Also the size and morphology of nickel Schiff base complex supported on boehmite (Ni-complex-boehmite **II**) were studied by TEM technique. As shown in Figure 1b, the unit cells of Ni-complex-boehmite **II** were obtained in cubic orthorhombic structures with dimensions of 45 and 120 nm. Also, the TEM image of the Ni-complex-boehmite **II** showed that particles have a regular geometric shape in comparison with nanoboehmite (Figure 1b). To investigate the characterization of these catalyst, a typical EDS spectrum taken from the Ni-complex-boehmite **I** that was shown in Figure 2. The EDS spectra at different points of the image confirm the presence of Ni in the prepared modified nanoparticles. The EDS spectrum shows the presence of C, O, N, Al, Si and Ni species in the catalyst (Figure 2).
Also, to extend the scope of catalysts characterization, we have determined the loading of Ni on boehmite nanoparticles, by ICP-OES technique. The Ni amount of the immobilized catalyst on boehmite nanoparticles was found to be 67.98 × 10^{-5} and 36.97 × 10^{-5} mol g^{-1} based on inductively coupled plasma atomic emission spectroscopy (ICP-OES) for catalyst **I** and **II** respectively.

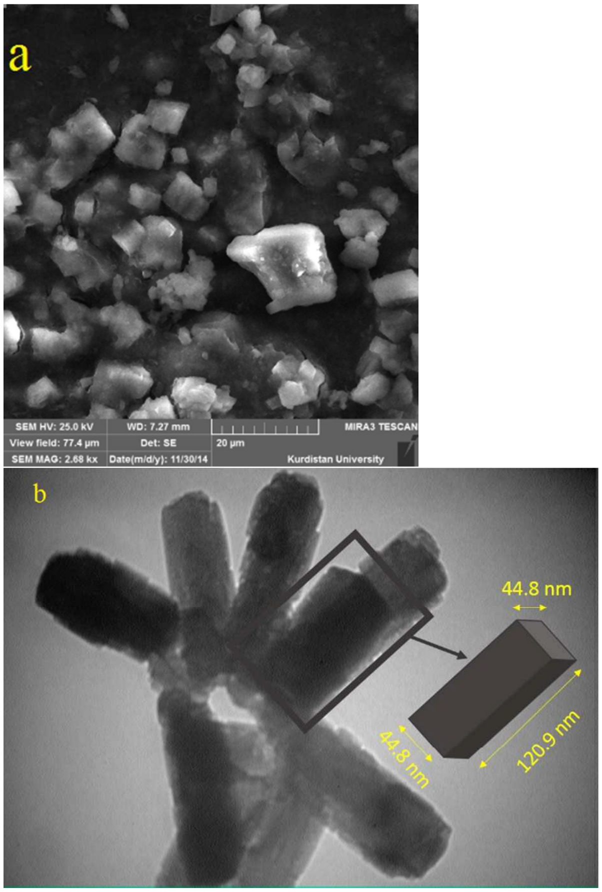

Figure 1. a) SEM image of boehmite nanoparticles and b) TEM image of Ni-complex-boehmite **II**.

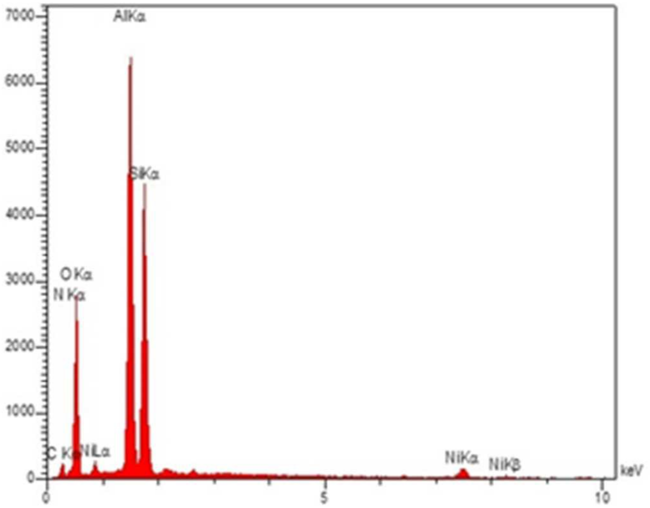

Figure 2. EDS spectrum of Ni-complex-boehmite **I**.

The XRD patterns of boehmite nanoparticles were shown in Figure 3. As it can be seen from Figure 3, the boehmite phase was identified from the XRD patterns by the peak positions at 14.40 (0 2 0), 28.41 (1 2 0), 38.55 (0 3 1), 46.45 (1 3 1), 49.55 (0 5 1), 51.94 (2 0 0), 56.02 (1 5 1), 59.35 (0 8 0), 65.04 (2 3 1), 65.56 (0 0 2), 68.09 (1 7 1), and 72.38 (2 5 1), which all peaks have been confirmed the crystallization of boehmite with an orthorhombic unit cell [6, 21].

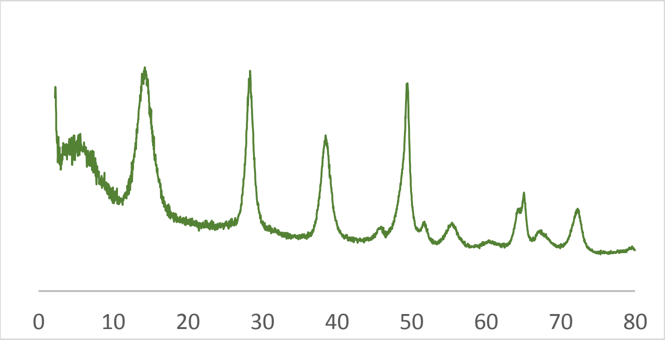

Figure 3. The XRD pattern of boehmite nanoparticles.

Immobilization of Schiff base complexes on functionalized nanoboehmite was inferred using TGA diagram. The TGA curve of nanoboehmite, boehmite coated by silica (boehmite-silica), Ni-complex-boehmite **I** and Ni-complex-boehmite **II** are shown in Figure 4. The weight loss at temperatures below 200 ºC is due to the removal of physically adsorbed solvents [22]. The boehmite and boehmite-silica are found to show a mass percentage loss of about 15% and 20% respectively, while the Ni-complex-boehmite **I** and Ni-complex-boehmite **II** has the greatest mass loss, at 50% and 45% respectively. On the basis of this result, the well grafting of nickel complexes on the boehmite nanoparticles is verified.

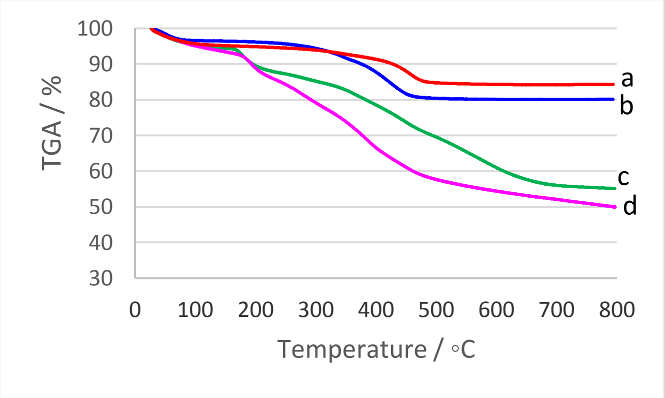

Figure 4. TGA diagram of a) nanoboehmite, b) boehmite coated by silica (boehmite-silica), c) Ni-complex-boehmite **II** and d) Ni-complex-boehmite **I**.

Successful functionalization of boehmite nanoparticles can be inferred from FT-IR spectra. Figure 5 shows FT-IR spectra for boehmite nanoparticles (a), boehmite-silica (b), boehmite-silica nanoparticle functionalized with APTES (BS-APTES) (c), Schiff base grafted on boehmite-silica (BS-Schiff base) **II** (d), BS-Schiff base **I** (f), Ni-complex-boehmite **II** (e) and Ni-complex-boehmite **I** (g). The FT-IR spectrum for the nanoboehmite shows a stretching vibration at 3086 and 3308 cm^{-1} from both symmetrical and asymmetrical modes of the O–H bonds, which are attached to the surface of boehmite nanoparticles. The structure of boehmite was confirmed *via* FT-IR by several peaks at 477, 613 and 735 cm^{-1}, which corresponds to the characteristic absorption of Al-O bonds [8]. Also, the nitrate impurity vibration at 1650 cm^{-1} and the vibrations of hydrogen bands OH…OH by two strong absorption bands at 1164 and 1069 cm^{-1} were observed in FT-IR spectrum [8, 10]. As it can be seen in Figure 5b-5g, the Si–O–Si bond's asymmetric stretching vibration and symmetric stretching vibration appear at 1072 cm^{-1} and 770 cm^{-1}, respectively, which indicates that the silica organic group has successfully coated the surface of boehmite nanoparticles [23]. In the FT-IR spectra of BS-APTES (Figure 5c), the presence of the anchored APTES was confirmed by C–H and N-H stretching vibrations that appear at 2931 cm^{-1} and 3097-3425 cm^{-1} respectively.

The FT-IR spectrum of BS-Schiff base **II** and BS-Schiff base **I** exhibits a weak bands at 1636 and 1635 cm^{-1} respectively, which attributed to the vibrations of C=N bands in the BS-Schiff bases that are absent in BS-APTES; while in the Ni-complex-boehmite **II** (Figure 5e) and Ni-complex-boehmite **I** (Figure 5g), these bands were shifted to lower frequency and appeared at 1628 and 1629 cm^{-1} respectively, which indicates the formation of Ni Schiff base complexes. C-O stretching vibrations show a peak at 1250-1300 cm^{-1} [24]. The stretching vibrations of phenolic C-O bonds of the BS-Schiff base spectrum, which was shifted to higher frequencies in the spectrum of the Ni-complex-boehmite, indicating that the electron density in the phenolic C-O bond was increased by the deprotonation and coordination of the phenolic oxygen [25].

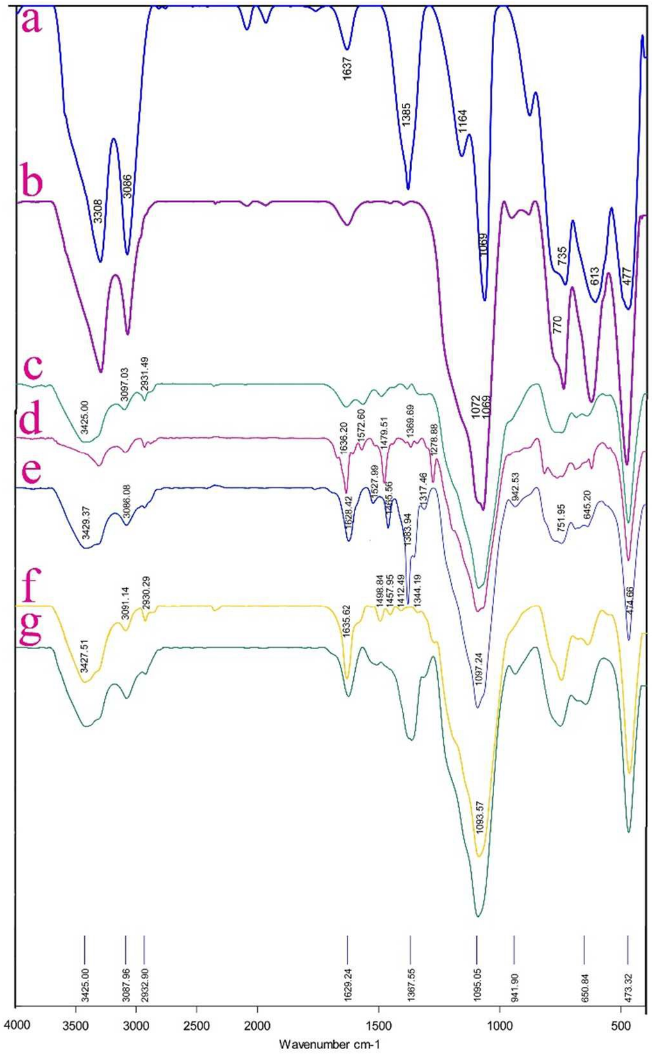

Figure 5. FT-IR spectra of boehmite nanoparticles (a), boehmite-silica (b), BS-APTES (c), BS-Schiff base **II** (d), BS-Schiff base **I** (f), Ni-complex-boehmite **II** (e) and Ni-complex-boehmite **I** (g).

The nitrogen adsorption-desorption isotherms of boehmite nanoparticles, Ni-complex-boehmite **I** and Ni-complex-boehmite **II** are shown in Figure 6. The hysteresis loop can be identified as type IV (definition by IUPAC), which is characteristic of mesoporous materials. It can be seen that the BET surface area and pore volume decrease after deposition of Ni metal on the support. The decrease in pore volume and surface area of Ni-complex-boehmite **I** and Ni-complex-boehmite **II** was attributed to the immobilization of organic layers and Ni-complex on the boehmite pores. These results are strong evidences that Ni-complex was bonded on the boehmite nanoparticles.

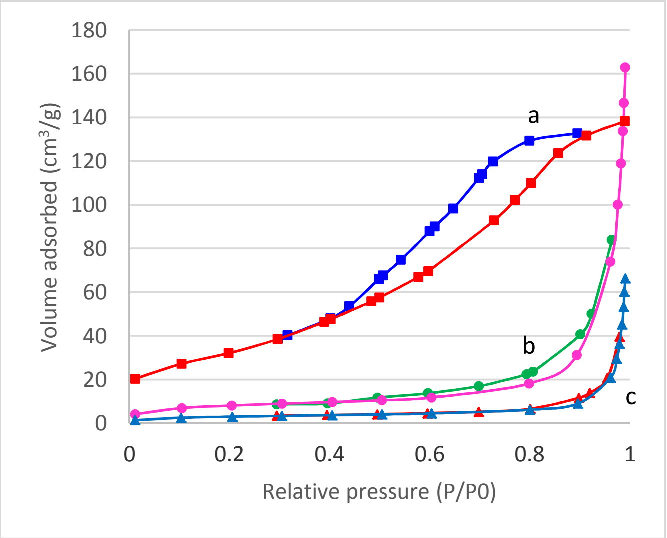

Figure 6. Nitrogen adsorption–desorption isotherms of samples: (a) boehmite nanoparticles, (b) Ni-complex-boehmite **I** and (c) Ni-complex-boehmite **II**.

The UV-DRS spectra of BS-Schiff base **I**, BS-Schiff base **II**, Ni-complex-boehmite **I** and Ni-complex-boehmite **II** are shown in Figure 7. The spectra for both ligands and both complexes show absorbance bands between 350-450 nm could be attributed to intra-ligand (π- π* and n- π*) charge transfer transition. In both Ni complexes two broad peaks between 500-650 nm assigned to d-d transition of Ni that are absent in BS-Schiff base **I** and **II**.

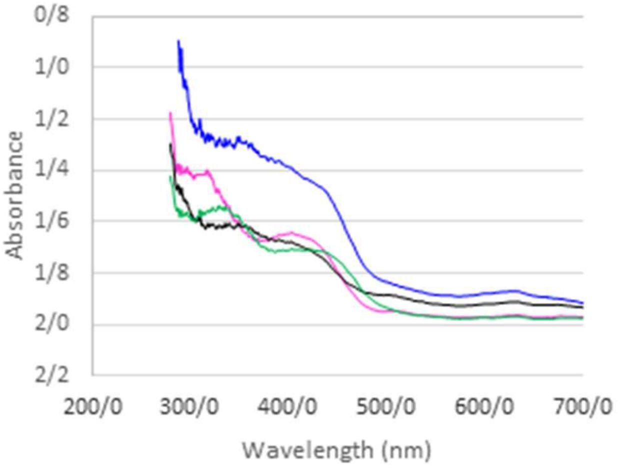

Figure 7. UV-DRS spectra for BS-Schiff base **I** (pink line), BS-Schiff base **II** (green line), Ni-complex-boehmite **I** (black line) and Ni-complex-boehmite **II** (blue line).

2.3 Catalytic study

In order to consider the catalytic activity of Ni-complex-boehmite (**I** and **II**), oxidation of sulfides to sulfoxides and also oxidative coupling of thiols into disulfides have been performed in the presence of these nanomaterials.

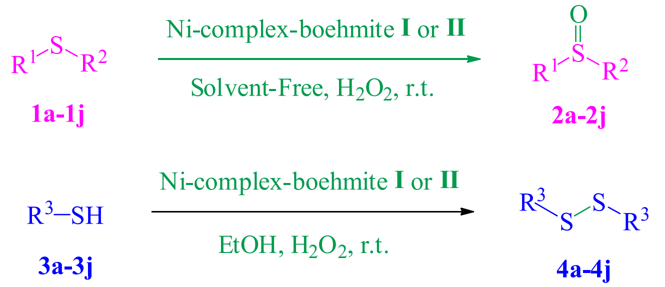

Scheme 2. Ni-complex-boehmite **I** or **II** catalyzed the oxidation of sulfides to sulfoxides and oxidative coupling of thiols into disulfides.

In order to optimize reaction conditions, we examined the oxidation of methylphenyl sulfide and oxidative coupling of naphthalene-2-thiol as a model compounds using H_2O_2 (0.4 mL) in various solvents and in the presence different amount of Ni-complex-boehmite **I** (Table 1). As shown in Table 1, in the oxidative coupling of naphthalene-2-thiol, the best results were obtained in ethanol using 0.004 gr (0.27×10^{-3} mol %) of Ni-complex-boehmite **I** at room temperature (Table 1, entry 5). Also the solvent-free condition in the presence of 0.003 gr (0.20×10^{-3} mol %) of Ni-complex-boehmite **I** was found to be ideal reaction conditions for the conversion of methylphenyl sulfide to the methylphenyl sulfoxide (Table 1, entry 12). Also we examined the oxidation of methylphenyl sulfide and oxidative coupling of naphthalene-2-thiol as a model compounds in various solvent and in the presence of different amount of Ni-complex-boehmite **II** using H_2O_2 (0.4 mL) (Table 2). The best results were obtained in the presence of 0.008 gr (0.29×10^{-3} mol %) of Ni-complex-boehmite **II** in the oxidation of methylphenyl sulfide and oxidative coupling of naphthalene-2-thiol respectively (Table 2, entries 3 and 13).

Table 1. Optimization of reaction conditions for the oxidation of methylphenyl sulfide and oxidative coupling of naphthalene-2-thiol in the presence of Ni-complex-boehmite **I** using H_2O_2 (0.4 mL).

Entry	Substrate	Solvent	Ni-complex-boehmite **I** (mg)	Time (min)	Yield (%)[a]
1	Naphthalene-2-thiol	Ethanol	-	15	0
2	Naphthalene-2-thiol	Ethanol	1	15	40
3	Naphthalene-2-thiol	Ethanol	2	15	70
4	Naphthalene-2-thiol	Ethanol	3	15	75
5	Naphthalene-2-thiol	Ethanol	4	15	90
6	4-Methylthiophenol	Acetonitrile	4	20	30
7	4-Methylthiophenol	CH_2Cl_2	4	20	40
8	4-Methylthiophenol	Ethyl acetate	4	20	50
9	4-Methylthiophenol	Water	4	20	40
10	Methylphenyl sulfide	Solvent-Free	0	15	0
11	Methylphenyl sulfide	Solvent-Free	1	15	30
12	Methylphenyl sulfide	Solvent-Free	3	15	97
13	Methylphenyl sulfide	Solvent-Free	5	15	50
14	Methylphenyl sulfide	Solvent-Free	7	15	60
15	Methylphenyl sulfide	Ethanol	3	15	55
16	Methylphenyl sulfide	Acetone	3	15	50
17	Methylphenyl sulfide	CH_2Cl_2	3	15	20
18	Methylphenyl sulfide	Ethyl acetate	3	15	70
19	Methylphenyl sulfide	n-Hexane	3	15	10

[a] Isolated yield.

Table 2. Optimization of reaction conditions for the oxidation of methylphenyl sulfide and oxidative coupling of naphthalene-

2-thiol in the presence of Ni-complex-boehmite **II** using H_2O_2 (0.4 mL).

Entry	Substrate	Solvent	Ni-complex-boehmite **II** (mg)	Time (min)	Yield (%)^a
1	Naphthalene-2-thiol	Ethanol	4	60	89
2	Naphthalene-2-thiol	Ethanol	6	60	92
3	Naphthalene-2-thiol	Ethanol	8	60	97
4	Naphthalene-2-thiol	Ethanol	10	50	94
5	4-Methylthiophenol	Acetonitrile	8	15	83
6	4-Methylthiophenol	CH_2Cl_2	8	15	65
7	4-Methylthiophenol	Ethyl acetate	8	15	81
8	4-Methylthiophenol	Water	8	15	20
9	4-Methylthiophenol	n-Hexane	8	15	62
10	Methylphenyl sulfide	Solvent-Free	2	95	93
11	Methylphenyl sulfide	Solvent-Free	4	95	95
12	Methylphenyl sulfide	Solvent-Free	6	95	94
13	Methylphenyl sulfide	Solvent-Free	8	95	98
14	Methylphenyl sulfide	Solvent-Free	10	95	92
15	Methylphenyl sulfide	CH_2Cl_2	8	95	53
16	Methylphenyl sulfide	Ethyl acetate	8	95	45
17	Methylphenyl sulfide	Ethanol	8	95	70
18	Methylphenyl sulfide	Acetonitrile	8	95	63
19	Methylphenyl sulfide	Water	8	95	42

[a] Isolated yield.

In order to show the role of boehmite and Ni during the reactions, oxidation of methylphenyl sulfide was examined in the presence of Ni-complex-boehmite **I** and **II** compared to alone boehmite and boehmite-silica. The results of this comparison are shown in Table 3. As shown in Table 3, the methylphenyl sulfoxide was obtained in 47 and 18% of yield in the presence of boehmite and boehmite-silica, respectively. Also to investigate the efficient catalytic activity of heterogeneous catalysts **I** and **II**, catalytic activity of corresponding homogeneous catalysts have been compared with these heterogeneous catalysts. As shown in Table 3, catalytic activity of heterogeneous and reusable catalysts are comparable with their homogeneous catalysts, because: 1) the boehmite was formed of nanometre-sized particles (Figure 1), which; when the size of the support is decreased to the nanometre scale, the surface area is substantially increased and the support can be completely dispersed in the reaction mixture (forming a homogenous emulsion). 2) High-surface-area of boehmite-silica nanoparticles including many hydroxyl groups leads to high catalyst loading capacity. Therefore, as shown in Table 3, these heterogeneous catalysts showed the advantages of both homogeneous (high catalytic activity) and heterogeneous (easy and rapid recoverability and recyclability) catalysts.

Table 3. The effect of boehmite or boehmite-silica and homogeneous catalyst **I** and **II** in comparison with Ni-complex-boehmite **I** and **II** in the oxidation of methylphenyl sulfide under optimized reaction conditions.

Entry	Substrate	Catalyst	Time (min)	Yield (%)^a
1	Methylphenyl sulfide	Boehmite nanoparticles	95	47^b
2	Methylphenyl sulfide	Boehmite-silica	95	18^b
3	Methylphenyl sulfide	Homogeneous catalyst **I**	80	98
4	Methylphenyl sulfide	Ni-complex-boehmite **I**	90	97
5	Methylphenyl sulfide	Homogeneous catalyst **II**	75	98
6	Methylphenyl sulfide	Ni-complex-boehmite **II**	95	98

[a] Isolated yield. [b] Yield was obtained by plate chromatography.

The generality of this approach has been demonstrated by a facile oxidation of various sulfides as shown in Table 4 (entries 1-10). As shown in Table 4, a variety of sulfides were successfully employed to prepare the corresponding sulfoxides. The sulfoxides were obtained in high yields. The experimental procedure is very simple. Therefore, the results revealed that this methodology is effective for the oxidation of a wide range of sulfides.

In order to explore the activity of these catalysts, various thiols including aromatic and aliphatic thiols with various functional groups were coupled in the presence of Ni-complex-boehmite under optimized conditions and the corresponding disulfide compounds obtained with good to excellent yields (Table 4, entries 11-20).

To show the chemoselectivity of the presented protocol, sulfides and thiols containing other functional groups were subjected to the oxidation reaction. These functional groups remained intact during the conversion of thiols to disulfides or sulfides into sulfoxides (Table 4, entries 5, 7 and 20). Because of mild conditions of described heterogeneous systems, there is no overoxidation to sulfone (for oxidation of sulfides) or thiosulfinates, disulfoxides, sulfinyl sulfones or disulfones (for the oxidative coupling of thiols) was observed.

Table 4. Oxidation of sulfides and oxidative coupling of thiols catalyzed by Ni-complex-boehmite **I** or **II**.

Entry	**Substrate**	**Product**	**Ni-complex-boehmite I**			**Ni-complex-boehmite II**			**Melting point (°C) [Ref.]**
			Time (min)	**Yield (%)^a**	**TOF (h^{-1})**	**Time (min)**	**Yield (%)^a**	**TOF (h^{-1})**	
1	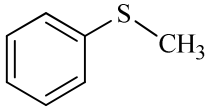	**2a**	90	97	323.33	95	98	213.43	Oil [17]
2	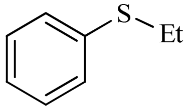	**2b**	270	80	88.89	330	95	59.56	Oil [26]
3	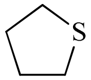	**2c**	5	95	5700	5	97	4013.79	Oil [15]
4	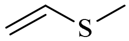	**2d**	25	97	1164	25	94	777.93	Oil [27]
5	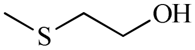	**2e**	10	80	2400	10	93	1924.14	Oil [15]

6	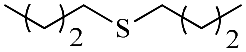	**2f**	195	95	146.15	150	97	133.79	Oil [16]
7	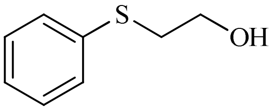	**2g**	10	90	2700	20	96	993.10	Oil [16]
8	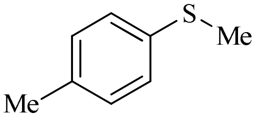	**2h**	160	85	159.37	130	98	155.97	Oil [27]
9	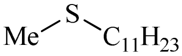	**2i**	180	80	133.33	150	99	136.55	62-65 [16]
10	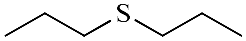	**2j**	60	85	424.99	70	99	292.61	Oil [16]
11	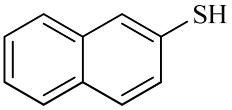	**4a**	15	90	133.33	60	97	334.48	134-136 [15]
12	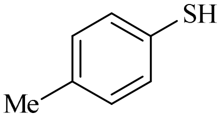	**4b**	20	95	1055.55	15	96	1324.14	35-37 [28]
13	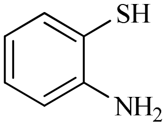	**4c**	50	85	377.77	60	91	313.79	82-84 [16]
14	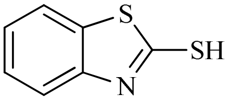	**4d**	80	97	269.44	120	92	158.62	174-176 [16]
15	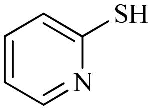	**4e**	60	85	314.81	60	98	337.93	55-57 [28]
16	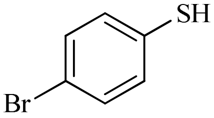	**4f**	150	80	118.52	120	96	165.52	88-90 [16]
17	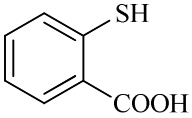	**4g**	120	90	166.67	120	97	167.24	275-279 [15]
18	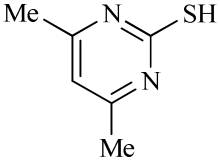	**4h**	60	95	351.85	25	98	811.03	159-161 [28]
19	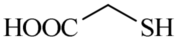	**4i**	60	80	296.30	70	94	277.83	Oil [15]
20	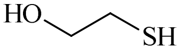	**4j**	30	95	703.703	25	96	794.48	Oil [16]

^{a}Isolated yield.

We have found that these catalysts were rapidly recovered and demonstrated remarkably excellent recyclability. In order to investigate this issue, the recyclability of these catalysts was examined in the oxidation of methyl phenyl sulfide and 4-methylthiophenol. After the completion of the reaction, the catalyst was separated by centrifuge technique. The remaining catalyst was washed with ethylacetate to remove residual product. Then, fresh substrates was added to the remaining catalyst without any activation and subjected to the next run. As shown in Figure 6, described catalysts can be recycled up to 5 runs without any significant loss of their catalytic activities.

In order to find the leaching of the catalysts, the amount of Ni in catalyst **II** were determined by ICP-OES after recycling. The amount of Ni in catalyst **II** was found to be 33.4 × 10^{-5} mol g^{-1} based on ICP-OES for catalyst **II** (9 %) after recycling. Therefore the catalyst can be recovered and reused without any significant leaching of Ni. Based on ICP-OES results, amount of Ni in the catalysts after recycle are comparable with the fresh catalyst.

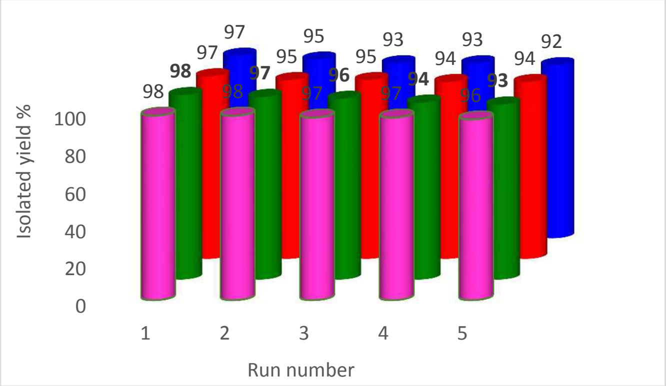

Fig 8. The recycling experiment of a) Ni-complex-boehmite **I** and b) Ni-complex-boehmite **II** in oxidation of methylphenyl sulfide and c) Ni-complex-boehmite **I** and d) Ni-complex-boehmite **II** in coupling of 4-methylthiophenol.

The efficiency of these nanocatalysts are demonstrated by comparison our result on the oxidation of methyl phenyl sulfide and oxidative coupling of 4-methylbenzenethiol with the previously reported procedures in the literature (Table 5). As it can be seen from this Table the good reaction time and higher yield than the other reported catalysts has been achieved. Also these new catalysts are comparable or may be better in terms of price, non-toxicity, stability and easy separation. In addition, these catalysts can be recycled at least 5 runs without any significant loss of their catalytic activity or metal leaching. Moreover, the mesoporous silica such as MCM-41, SBA-15 or some nanoparticles such as TiO_2 NPs, which have been used as catalyst support in the organic reactions, requires high temperature for calcination and a lot of time and tedious conditions to prepare. Also some of previously reported catalysts such as heteropolyacids, ionic liquids or some polymers are more expensive. Also preparation of boehmite nanoparticles was not air, or moisture sensitive, therefore this nanomaterial was prepared in water at room temperature without inert atmosphere.

Table 5. Comparison of Ni-complex-boehmite **I** and **II** for the oxidation of methyl phenyl sulfide and oxidative coupling of 4-methylbenzenethiol with previously reported procedure.

Entry	Substrate	Catalyst	Time (min)	Yield ^{a} (%) [Reference]
1	Ph-SCH_3	NBS	270	93 [29]
2	Ph-SCH_3	Ni-salen-MCM-41	156	95 [30]
3	Ph-SCH_3	Cd-salen-MCM-41	150	98 [30]
4	Ph-SCH_3	TsOH	240	88 [31]
5	Ph-SCH_3	$VO_2F(dmpz)_2$	300	95[32]
6	Ph-SCH_3	Heterocyclic amine salts of Keggin heteropolyacids	120	95 [33]
7	Ph-SCH_3	polymer-anchored Cu(II)	180	90 [34]
8	Ph-SCH_3	SiO_2–W_2–Im	150	91.9 [37]
9	Ph-SCH_3	Ni-complex-boehmite **I**	90	97 [This work]
10	Ph-SCH_3	Ni-complex-boehmite **II**	95	98 [This work]
11	*p*-MePh-SH	CuI/Cs_2CO_3/1,10-phen	720	97 [19]
12	*p*-MePh-SH	Ni-salen-MCM-41	25	95 [30]
13	*p*-MePh-SH	Cd-salen-MCM-41	20	97 [30]
14	*p*-MePh-SH	Fe NPs@SBA-15	45	94 [36]
15	*p*-MePh-SH	[bmim][$SeO_2(OCH_3)$]	120	99 [37]
16	*p*-MePh-SH	STA-RGO	25	85 [38]
17	*p*-MePh-SH	Mn–ZSM-5	360	83.2 [39]
18	*p*-MePh-SH	Ni-complex-boehmite **I**	20	95 [This work]
19	*p*-MePh-SH	Ni-complex-boehmite **II**	15	96 [This work]

^{a} Isolated yield.

3 Conclusions

In summary, we have demonstrated that Ni-complex-boehmite (**I** and **II**) can be used as a green, efficient and reusable nanocatalysts for the oxidation of sulfides to sulfoxides and oxidative coupling of a wide range of thiols into disulfides using H_2O_2 at room temperature. The advantages of this protocol are the use of commercially available materials, eco-friendly conditions, cheap oxidant, the mild reaction conditions, operational simplicity, practicability and good to high yields of reactions. Also the catalyst can be reused for 5 times without any significant loss of its activity. More importance, nanoboehmite is new support for the heterogenization of homogeneous catalysts, which has several advantages such as high surface area, easily and readily available material to prepare, thermal and mechanical stability, ease of surface modification, easy and inexpensive procedure of preparation.

4 Experimental

4.1. Preparation of the Ni-complex-boehmite

The solutions of 6.490 g NaOH in 50 mL of distilled water was added to the solutions of $Al(NO_3)_3.9H_2O$ (20 g) in 30 mL distilled water drop wise under vigorous stirring. The resulting milky mixture was subjected to mixing in the ultrasonic bath for 3 h at 25 ºC. The resulted nanoboehmite was filtered and washed by distilled water and were kept in the oven at 220 ºC for 4 h.

The obtained boehmite nanoparticles (1 g) were dispersed in water (10 mL) and ethanol (50 mL) by sonication for 30 min. Under continuous stirring, PEG (5.36 g), ammonia solution (10 mL) and TEOS (2 mL) were respectively added into the suspension, and continuously reacted for 38 h at room temperature. Then, the product (boehmite-silica) was filtered and washed with ethanol and distilled water, the obtained boehmite-silica was dried at room temperature.

The obtained boehmite-silica (1.5 g) was dispersed in 100 mL dry n-hexane solution by sonication for 30 min, then (3-aminopropyl)-trimethoxysilane (APTES) (2.5 mL) was added to the reaction mixture. The reaction mixture was stirred at 40 ºC for 8 h. Subsequently, nanoparticles have been isolated by simple filtration and washed with ethanol. The nanoparticles (BS-APTES) were dried at room temperature. In order to prepare BS-Schiff base, the above mentioned solid (1 g) was refluxed with salicylaldehyde (1 mmol) or 5-bromosalicylaldehyde (1 mmol) in ethanol for 8h. The resulting solid (BS-Schiff base) was separated using filtration, washed with ethanol and dried at room temperature. Finally, for the preparation of Ni-complex-boehmite, the BS-Schiff base (1.0 g) was dispersed in ethanol and was mixed with 1.0 mmol of $Ni(NO_3)_2.6H_2O$. The mixture was stirred at 80 ºC for 15 h. The solid product (Ni-complex-boehmite) was obtained after washing with ethanol and drying at 50 ˚C.

4.2 General procedure for the oxidation of sulfides to sulfoxides

A mixture of sulfide (1 mmol), H_2O_2 (0.4 mL) and Ni-complex-boehmite **I** (0.003 g, 0.20 × 10^{-3} mol%) or Ni-complex-boehmite **II** (0.008 g, 0.29 × 10^{-3} mol%) was stirred at room temperature under solvent-free condition and the progress of the reaction was monitored by TLC. After completion of the reaction, catalyst was separated using filtration and washed with ethyl acetate, and the product was extracted with ethyl acetate. The organic layer was dried over anhydrous Na_2SO_4 (1.5 g). Finally, the organic solvents were evaporated, and products were obtained in good to high yield.

4.3 General procedure for the oxidative coupling of thiols into disulfides

Ni-complex-boehmite **I** (0.004 g, 0.27×10^{-3} mol%) or Ni-complex-boehmite **II** (0.008 g, 0.29×10^{-3} mol%) was added to a mixture of thiol (1 mmol) and H_2O_2 (0.4 mL) in ethanol (3 mL). Then the mixture was stirred for the appropriate time at room temperature. The progress of reaction was monitored by TLC. After completion of the reaction, the catalyst was separated by filtration and the mixture was washed with ethyl acetate. The product was extracted with ethyl acetate. The organic layer was dried over anhydrous Na_2SO_4 (1.5 g). The products were obtained in good to high yield.

4.4 Selected spectral data

Tetrahydrothiophene 1-oxide (Table 4, entry 3): ^{1}H NMR (400 MHz, $CDCl_3$): δ = 2.27 (t, *J*= 7.5 Hz, 2H), 3.07 (t, *J*= 7.6 Hz, 2H) ppm.
Methyl(p-tolyl)sulfane (Table 4, entry 8): ^{1}H NMR (400 MHz, $CDCl_3$): δ = 2.22 (s, 3H), 2.57 (s, 3H), 7.19 (d, *J*= 3.2 Hz, 2H), 7.39 (d, *J*= 3.2 Hz, 2H) ppm.
1-(Propylsulfinyl)propane (Table 4, entry 10): ^{1}H NMR (400 MHz, $CDCl_3$): δ = 1.11 (t, *J*= 6 Hz, 6H), 1.84-1.93 (m, 4H), 2.65-2.97 (m, 4H) ppm.
1,2-di(naphthalen-2-yl)disulfane (Table 4, entry 11): ^{1}H NMR (400 MHz, $CDCl_3$): δ = 7.49 (m, 4H), 7.63 (m, 2H), 7.74 (m, 2H), 7.80 (m, 4H), 8.11 (s, 2H) ppm.
1,2-di-p-tolyldisulfane (Table 4, entry 12): ^{1}H NMR (400 MHz, $CDCl_3$): δ = 2.35 (s, 6H), 7.12 (d, *J*= 7.9 Hz, 4H), 7.43 (d, *J*= 7.89 Hz, 4H) ppm.
1,2-bis(benzo[d]thiazol-2-yl)disulfane (Table 4, entry 14): ^{1}H NMR (400 MHz, $CDCl_3$): δ = 7.36 (t, *J*= 3.2 Hz, 2H), 7.48 (t, *J*= 3.2 Hz, 2H), 7.80 (d, *J*= 3.2 Hz, 2H), 7.94 (d, *J*= 3.2 Hz, 2H) ppm.
1,2-bis(4-bromophenyl)disulfane (Table 4, entry 16): ^{1}H NMR (400 MHz, $CDCl_3$): δ = 7.35 (d, *J*= 8.2 Hz, 4H), 7.42 (t, *J*= 8.2 Hz, 4H) ppm.
1,2-bis(4,6-dimethylpyrimidin-2-yl)disulfane (Table 4, entry 18): ^{1}H NMR (400 MHz, $CDCl_3$): δ = 2.40 (s, 12H), 6.74 (s, 2H) ppm.
2,2'-Disulfanediyldiethanol (Table 4, entry 20): ^{1}H NMR (400 MHz, $CDCl_3$): δ = 2.60 (br, 2H), 2.89 (t, *J*= 5.6 Hz, 4H), 3.93 (t, *J*= 5.6 Hz, 4H) ppm.

Acknowledgements

This work was supported by the research facilities of Ilam University, Ilam, Iran.

References

1. V. Polshettiwar, R.S. Varma, *Green Chem.* 2010, **12**, 743.
2. A. Ghorbani-Choghamarani, F. Nikpour, F. Ghorbani, F. Havasi, *RSC Adv.* 2015, **5**, 33212.
3. S. Shylesh, V. Schunemann, W.R. Thiel, *Angew. Chem. Int. Ed.* 2010, **49**, 3428.
4. Y. Zhu, L.P. Stubbs, F. Ho, R. Liu, C.P. Ship, J.A. Maguire, N.S. Hosmane, *ChemCatChem.* 2010, **2**, 365.
5. M. Hajjami, B. Tahmasbi, *RSC Adv.* 2015, **5**, 59194.
6. K. Bahrami, M.M. Khodaei, M. Roostaei, *New J. Chem.* 2014, **38**, 5515.
7. Z. Wu, Y. Mao, M. Song, X. Yin, M. Zhang, *Catal. Commun.* 2013, **32**, 52.
8. V. Vatanpour, S.S. Madaenia, L. Rajabi, S. Zinadini, A.A. Derakhshan, *J. Membr. Sci.* 2012, **401-402**, 132.
9. M.B. Gholivand, G. Malekzadeh, A.A. Derakhshanc, *Sensor. Actuat. B Chem.* 2014, 201, 378.
10. L. Rajabi, A.A. Derakhshan, *Sci. Adv. Mater.* 2010, **2**, 163.
11. Z. Abbasi, M. Behzad, A. Ghaffari, H.G. Amiri Rudbari, G. Bruno, Inorganica. Chimica. Acta. 2014, 414, 78.
12. F. Dehghani, A.R. Sardarian, M. Esmaeilpour, *J. Organomet. Chem.* 2013, **743**, 87.
13. E.G. Bowes, G.M. Lee, C.M. Vogels, A. Decken, S.A. Westcott, *Inorg. Chim. Acta.* 2011, **377**, 84.
14. Q. Zeng, W. Weng, X. Xue, *Inorg. Chim. Acta.* 2012, **388**, 11.
15. A. Ghorbani-Choghamarani, Z. Darvishnejad, M. Norouzi, *Appl. Organometal. Chem.* 2015, **29**, 170.
16. A. Ghorbani-Choghamarani, Z. Darvishnejad, B. Tahmasbi, *Inorg. Chim. Acta.* 2015, **435**, 223.
17. M. Hajjami, S. Rahmani, *J. Porous. Mater.* 2015, **22**, 1265.
18. Z. Zhang, W. Li, J. Liu, X. Chen, Y. Bu, *J. Organomet. Chem.* 2012, **706-707**, 89.
19. Y. Liu, H. Wang, C. Wang, J.P. Wan, C. Wen, *RSC Adv.* 2013, **3**, 21369.
20. H. Zhang, G. Wang, *Tetrahedron Lett.* 2014, **55**, 56.
21. H. Liu, J. Deng, W. Li, *Catal. Lett.* 2010, **137**, 261.
22. B. Atashkar, A. Rostami, B. Tahmasbi, *Catal. Sci. Technol.* 2013, **3**, 2140.
23. F. Havasi, A. Ghorbani-Choghamarani, F. Nikpour, *New J. Chem.* 2015, **39**, 6504.
24. F. Dehghani, A.R. Sardarian, M. Esmaeilpour, *J. Organomet. Chem.* 2013, **743**, 87.
25. S.A. Beyramabadi, A. Morsali, S.H. Vahidi, M.J. Khoshkholgh, A.A. Esmaeili, *J. Struct. Chem.* 2012, **53**, 460.
26. A. Ghorbani-Choghamarani, G. Azadi, B. Tahmasbi, M. Hadizadeh-Hafshejani, Z. Abdi, *Phosphorus Sulfur Silicon Relat. Elem.* 2014, **189**, 433.
27. M. Nikoorazm, A. Ghorbani-Choghamarani, H. Goudarziafshar, *Bull. Korean Chem. Soc.* 2009, **30**, 3120.
28. M. Nikoorazm, A. Ghorbani-Choghamarani, F. Ghorbani, H. Mahdavi, Z. Karamshahi, *J. Porous. Mater.* 2015, **22**, 261.
29. B. Karimi, D. Zareyee, *J. Iran. Chem. Soc.,* 2008, **5**, Sl03.
30. M. Nikoorazm, A. Ghorbani-Choghamarani, H. Mahdavi, S.M. Esmaeili, *Microporous and Mesoporous Mater.* 2015, **211**, 174.
31. B. Yu, C.X. Guo, C.L. Zhong, Z.F. Diao, L.N. He, *Tetrahedron Lett.* 2015, **55**, 1818.
32. S. Hussain, D. Talukdar, S.K. Bharadwaj, M.K. Chaudhuri, *Tetrahedron Lett.* 2012, **53**, 6512.
33. A.G. Sathicq, G.P. Romanelli, V. Palermo, P.G. Vazquez, H.J. Thomas, *Tetrahedron Lett.* 2008, **49**, 1441.
34. S.M. Islam, A.S. Roy, P. Mondal, K. Tuhina, M. Mobarak, J. Mondal, *Tetrahedron Lett.* 2012, **53**, 127.
35. S. Xian-Ying, W. Jun-Fa, *J. Mol. Catal. A: Chem.* 2008, **280**, 142.
36. F. Rajabi, T. Kakeshpour, M.R. Saidi, *Catal. Commun.* 2013, **40**, 13.
37. S. Thurow, V.A. Pereira, D.M. Martinez, D. Alves, G. Perin, R.G. Jacob, E.J. Lenardão, *Tetrahedron Lett.* 2011, **52**, 640.
38. S.V. Nipane, M.G. Mali, G.S. Gokavi, *Ind. Eng. Chem. Res.* 2014, **53**, 3924.
39. A.K. Patra, A. Dutta, M. Pramanik, M. Nandi, H. Uyama, A. Bhaumik, *ChemCatChem.* 2014, **6**, 220.

Graphical Abstract

Nickel Schiff-base complexes immobilized on boehmite nanoparticles and their application in the oxidation of sulfides and oxidative coupling of thiols as novel and reusable catalysts

Arash Ghorbani-Choghamarani, Bahman Tahmasbi, Fatemeh Arghand and Sara Faryadi

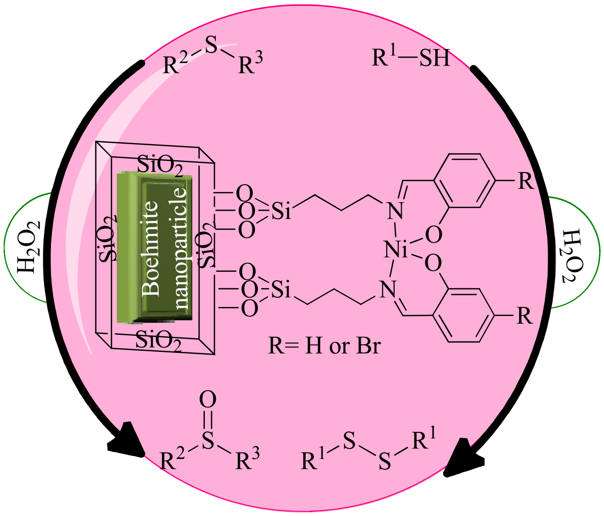

Ni-complex-boehmite was prepared in water at room temperature using commercially available materials and applied as efficient nanocatalyst in the oxidation of sulfides and thiols.